Submitted to the 29th International Conference on High-Energy Physics ICHEP98,
Vancouver, Canada, July 1998

Measurement of the Baryon-Antibaryon Asymmetry in Photoproduction at HERA

H1 Collaboration

Abstract

Results are given for the inclusive photoproduction of protons and antiprotons measured with the H1 detector in ep collisions at HERA. The particle identification is based on $\mathrm{d}E/\mathrm{d}x$ measurement. A non-vanishing baryon asymmetry has been observed in the photon hemisphere. The baryon asymmetry is studied as a function of the charged particle multiplicity.

Abstract: 556
Parallel sessions: 5
Plenary sessions: 7

1 Introduction

The existence of baryons, baryon number conservation and baryon asymmetry in the universe are phenomena of fundamental importance in the modern physical picture of the world. The understanding of these phenomena is closely related to the question about the carrier of the baryon identity (the baryon number). In the quark–parton model any quark carries $1/3$ of the baryon number unit. The baryons appear as particles built up from the three constituent quarks. When the baryon gets destroyed by inelastic scattering on other particles, the quarks can recombine into another baryon at a new position in the momentum space. The question we would like to address in the present paper is how far the baryon number can be transferred in the momentum (or rapidity) space in inelastic scattering.

Within a widely spread approach the baryon acts as a diquark–quark system. In the collision of baryons the diquarks take a large part of the projectile momentum and give rise to leading baryon production in the projectile fragmentation region. In this approach baryon number transfer over large rapidity intervals is strongly suppressed. The diquark model is very illustrative and describes the bulk of the data on leading baryon production.

However, within this approach, in which the carrier of the baryon number is the diquark, there are also measurements which are difficult to explain: the energy dependence of the $p\bar{p}$ annihilation cross section [1], the rapidity distributions of the net baryon number $(p - \bar{p})$ at the CERN ISR [2, 3] and in high energy heavy ion collisions [4], and reactions with a final state leading baryon having valence quarks different from the quark content of the baryonic projectile. These measurements indicate that the baryon number can be transported with high probability over a large rapidity gap. To describe such data two new mechanisms of baryon number transfer have been suggested [5, 6]: single-quark and gluonic mechanisms. Both mechanisms imply a break up of the diquark. The first one is founded on calculations and explains well the ISR data as well as the stopping of the proton in heavy ion collisions [5, 7]. The gluonic mechanism is so far only a rough estimate as there are no data available to compare with. This mechanism predicts an asymptotic non-vanishing annihilation cross section and no suppression for baryon number transfer over large rapidity intervals.

The HERA data on high energy photon–proton collisions offer a unique opportunity to study the mechanisms of baryon number transfer. The asymmetry in the beam energies makes it possible to study baryon production in the photon hemisphere up to 8 units of rapidity distance from the leading baryon production region. It has been shown in [8] that at such large rapidity intervals the gluonic mechanism gives a dominant contribution to baryon number transfer. The authors of [8] proposed that the baryon production asymmetry to be measured at HERA in the photon hemisphere, defined as

$$A_B = 2 \cdot \frac{N_p - N_{\bar{p}}}{N_p + N_{\bar{p}}}, \tag{1}$$

where N_p, $N_{\bar{p}}$ are the numbers of protons and antiprotons produced in a given rapidity interval. The calculations made in [8] predict the asymmetry A_B in the photon hemisphere at HERA to be as big as about 7%, which is in reach with the presently available statistics collected by experiments at the HERA ep collider. It is interesting to note that a surplus of protons over antiprotons has been observed in the photon hemisphere in μH_2 and μD_2 collisions by the EMC experiment [9] at low energy. However, at low collision energy the available rapidity space is small and does not allow the baryon number to be transferred over large distances. In this paper we describe the first measurement of the baryon asymmetry in photon–proton collisions at an average center of mass energy $W = 200$ GeV using the H1 detector.

2 Experimental Procedure

The measurements presented here are based on the H1 data taken during 1996 and correspond to an integrated luminosity of about 8 pb^{-1}.

The H1 detector is described in detail elsewhere [10]. A brief account of the components that are most relevant to the present analysis is given here. These are the positron tagger, the central tracker, the backward calorimeter (Spacal) and the liquid argon (LAr) calorimeter. The direction of the z-axis is chosen to be along the proton beam direction. The polar angle θ is defined with respect to the z-axis and pseudorapidity is given by $\eta = -\ln(\tan(\theta/2))$.

The positron tagger, located at $33\,$m from the interaction point in the positron direction, measures the energy of the scattered positron and, in conjunction with a photon detector, the luminosity by exploiting the Bethe-Heitler process $ep \to ep\gamma$. The photon detector is located 100 m from the interaction point, in the positron direction.

The central track detector consists of inner and outer concentric central jet chambers (CJC), multi-wire proportional chambers for triggering purposes and two additional drift chambers which measure accurately the z-coordinate. The pseudorapidity range covered by the central track detector is $|\eta| < 1.5$. The CJC has 56 sensitive wire layers and is filled with a gas mixture of Ar-$Ethane$ $(50\% : 50\%)$ at atmospheric pressure. The track detector is placed inside an uniform magnetic field of 1.15 T. The CJC measures the transverse momentum and the specific energy loss $\mathrm{d}E/\mathrm{d}x$ of charged particles. The transverse momentum resolution is $\sigma_{p_t}/p_t \approx 0.009{\cdot}p_t[GeV]{\oplus}0.015$. The typical $\mathrm{d}E/\mathrm{d}x$ resolution is $\sigma(\mathrm{d}E/\mathrm{d}x)/(\mathrm{d}E/\mathrm{d}x) \approx 7.5\%$ for 56 charge samples on a minimum ionizing track.

The LAr and Spacal calorimeters surround the tracking system and cover the angular range $4^\circ < \theta < 154^\circ$ and $153^\circ < \theta < 177.8^\circ$ respectively. Here the calorimeters are only used to identify and reject background events resulting from beam–gas interactions.

Photoproduction events are selected by requiring the presence of a scattered positron in the small angle positron tagger. For these events the photon virtuality is restricted to $Q^2 < 10^{-2}$ GeV^2. The energy measured by the positron tagger is used in the determination of the total γp collision energy W. In the main detector γp events are triggered by demanding, in addition to a signal in the positron tagger, the presence of at least three tracks in the CJC.

In order to reduce the non-ep background contamination and to ensure good reconstruction of the event kinematics, the following selection criteria have been applied for this analysis:

- Photoproduction events are required to lie within the interval $150 < W < 260$ GeV. This corresponds to an average photon–proton collision energy of $W = 200$ GeV.
- The trigger conditions are verified by selecting only multi–hadron events with more than two reconstructed tracks pointing to the common event vertex.
- In order to suppress random coincidences between the high rate Bethe–Heitler events and beam–gas background in the main H1 detector, events were rejected if a photon with energy $E_\gamma > 2\ \mathrm{GeV}$ was detected in the photon tagger.
- The event vertex reconstructed from the tracks of charged particles was required to lie within ± 30 cm of the nominal $z-$position of the interaction point, corresponding to about 3σ cut on the interaction region defined by the longitudinal size of the proton bunch.

Fig. 1 (a,b) shows the distribution of the reconstructed $z-$position and the radius of the event vertex. The peak around $R_{vertex} = 4.5$ cm corresponds to a small fraction of events resulting from off–beam particle interactions with the material of the beam tube. The events with $R_{vertex} > 2.5$ cm were removed.

In total about $3.5 \cdot 10^6$ events satisfy the above selection criteria. The selected events contain both the primary particles originating from the common event vertex, and secondary particles resulting from decays and rescattering in the detector volume. Fig. 1 (c,d) shows distributions of track distance of closest approach to a common vertex in the plane transverse to the beam direction (DCA) and along the z-direction (Δz), respectively. The primary particles give rise to the peaks around zero, while the background tracks are randomly distributed around the actual event vertex position. For the present analysis we consider tracks with $|DCA| < 7$ cm and $|\Delta z| < 7$ cm only.

In order to ensure high efficiency for the track reconstruction and particle identification the tracks for the analysis are selected within the angular interval $|\cos(\theta)| < 0.8$, which corresponds to the pseudorapidity range $|\eta_{lab}| < 1$. For each track a minimum of 20 jet chamber hits is required, usable for the determination of the energy loss $\mathrm{d}E/\mathrm{d}x$. The measurement of the particle ionization loss is based on a likelihood method [11]. In Fig. 2(a) the measured ionization energy loss in units of the ionization energy for a minimally ionizing particle (MIP) is shown versus the momentum of the particle. The following additional requirements are applied to the reconstructed tracks in order to optimize the proton and antiproton measurements:

- To isolate the protons from minimum ionizing particles the measured energy loss $\mathrm{d}E/\mathrm{d}x$ has to be greater than $2 \times (\mathrm{d}E/\mathrm{d}x)_{MIP}$.
- To keep high efficiency of the proton reconstruction the momentum interval is chosen to be $0.3 < p < 0.6$ GeV/c.

A clear particle separation is observed under the above conditions, as demonstrated in Fig. 2(b). The mass of the particle, M, is reconstructed from the simultaneous measurement of the momentum and the energy loss of the track. Positive particles are shown by the histogram, while negative particles are given by points with error bars. The peak around $\log_{10}(M) \approx 0$ corresponds to the (anti)protons, and the peak at $\log_{10}(M) \approx -0.3$ corresponds to the kaons. A sizable excess of protons over antiprotons is observed. Several sources of background contribute to this excess:

- A certain fraction of hadrons resulting from the ep collision interacts strongly with material of the beam tube or CJC walls and produces events containing spallation protons from the material. The reconstructed tracks from these protons have a broad distribution in their DCA with sharp edges at the radius of the beam tube $R \approx 4.5$ cm. In Fig. 3(a) the DCA distribution is shown for the identified protons in the data. This distribution has a narrow peak around $DCA = 0$ and a broad plateau resulting from secondary interactions in the detector material. A Monte Carlo simulation of γp events qualitatively reproduces the observed plateau of secondary particles in the DCA distribution. Fig.3(b) shows the result of a Monte Carlo calculation for protons produced in the material of the beam pipe. This distribution, contrary to the behaviour of protons produced in ep–interactions, has no peak at $DCA = 0$. To reduce this source of background only multi-hadron events are accepted which contain exactly one proton or one antiproton. This condition, being symmetric for protons and antiprotons, reduces background from secondary protons by more than 60%.

- Accidental coincidence of positron tagger signals with events resulting from the interactions of beam particles with the residual gas within the nominal ep interaction region. Such events are characterized both by the low energy protons produced in nuclear spallation reactions and by particular event topologies. For p–gas events there is very little energy deposited in the Spacal calorimeter, E_{back} (backward with respect to the proton beam direction). Similarly, for e–gas interactions no energy is deposited in the angular interval $\theta < 30°$ in the LAr calorimeter, E_{forw}. The distributions of E_{back} and E_{forw} are shown in Fig. 3(c,d). To suppress the contribution of beam–gas events to the multi–hadron event sample $E_{back} > 1$ GeV and $E_{forw} > 2$ GeV are required in the further analysis. The latter condition on E_{forw} removes also diffractive rapidity gap events. In order to estimate the suppression power of this requirement, a sample of multi–hadron events was selected with the reconstructed z–position of the vertex outside the nominal interaction region $30 < |z_{vertex}| < 40$ cm and with at least two identified protons pointing to the common event vertex. This event sample contains about 300 events and is dominated by beam-gas induced background. No event was found with two or more identified antiprotons. After applying the calorimeter requirements to the selected events only 9 events survive. This gives an estimate for the suppression factor of 0.03 ± 0.01.

- A small fraction of protons produced in the material of the outer tracker wall and scattered back into the sensitive volume of the CJC is reconstructed with opposite sign of the charge and contributes to the sample of the antiprotons. These particles have a random distribution in DCA.

Fig. 4 shows the mass spectrum measured for tracks with $|DCA| < 1$ cm, after background suppression. Positively charged particles are shown by the histogram, while negative particles are given by full circles with error bars. A remarkable agreement is observed in the number of reconstructed K^+ and K^-. The number of protons is significantly larger than the number of antiprotons. In the next section the final step to remove residual background from the proton sample is discussed.

3 Results

In Fig. 5 the DCA distributions are shown for those positive and negative particles for which the value of $\log_{10}(M)$ lies within a window of ± 0.1 around the nominal value for the proton mass. The DCA distributions are fitted to a sum of three Gaussians describing the primary protons produced at the main event vertex and a polynomial function representing the background from secondary particles produced in the detector material. The results of the fits are also shown in Fig. 5. The numbers of protons and antiprotons under the Gaussians are found to be $N_p = 43980 \pm 550$ and $N_{\bar{p}} = 39449 \pm 201$, respectively. However, the resulting number of protons N_p still contains a small fraction of residual beam gas background. To estimate this background contribution, we repeat the described fit of the DCA spectra for the beam-gas background enriched event sample with a requirement on the calorimeter energies E_{back} and E_{forw} to be complementary to that used for the physics event selection. The numbers of protons and antiprotons obtained from the fit in this background event sample are $N'_p = 16196$ and $N'_{\bar{p}} = 9452$ respectively. Assuming that the difference $N'_p - N'_{\bar{p}}$ is dominated by the background protons and applying the background suppression factor of the calorimeter requirements discussed in the previous section, one can estimate the residual contribution of beam–gas events to the selected physics event sample. The residual background contribution to the number of protons was found to be $N_{bgr} = 200 \pm 60$. Thus the visible asymmetry of protons and antiprotons is

$$A_B^{obs} = 2 \cdot \frac{N_p - N_{bgr} - N_{\bar{p}}}{N_p - N_{bgr} + N_{\bar{p}}} = (10.5 \pm 1.5)\%. \tag{2}$$

The measured value of the baryon asymmetry A_B^{obs} has to be corrected for different absorption probabilities of protons and antiprotons in the detector material they transverse before entering the CJC sensitive volume. This material is dominated by the 2 mm thick Aluminum beam tube. The calculations made using the GEANT Monte Carlo program [12] reduce the obtained value of the baryon asymmetry down to 8.0%. The absorption cross sections for p and $\bar{p}$ used in the GEANT program have been checked versus available data [13] in the momentum interval corresponding to the present analysis.

A potential source of systematic error in A_B is the difference in reconstruction efficiency for negative and positive particles. The Monte Carlo calculations do not reveal any difference within 0.5% accuracy. To verify this result with the data the number of reconstructed π^+ and π^- are compared within the momentum and angular interval used in the present analysis. The pions are identified as particles with measured energy losses below $1.5 \cdot (\mathrm{d}E/\mathrm{d}x)_{MIP}$ value. In Fig. 6 the measured $\mathrm{d}E/\mathrm{d}x$ and momentum distributions are compared for positive and negative pions. The charge asymmetry in the number of measured pions A_π, defined analogously to the baryon asymmetry, was found to be $(0.75 \pm 0.40)\%$. A small admixture of kaons in the selected pion sample does not affect the obtained value of A_π. A conservative estimate of this part of the systematic error is 1.5%.

Variations of the cuts used in the proton selection and background suppression and of the parametrisation of the function to fit the DCA distributions resulted in an additional systematic error of 1.0% to the value of A_B. It is worthwhile to mention among the variations of selection criteria the following:

- The reconstructed event vertex was constrained to be within ± 10 cm of the nominal $z-$position of the interaction point. This requirement reduces strongly the relative contribution from the beam–gas induced background events, which have a flat distribution of the event vertex along the z–axis.
- The minimum number of hits on a track was increased from 20 to 30.
- The size of the window around the nominal $\log_{10}(M)$ value of the proton was varied between ± 0.07 and ± 0.13.
- The requirement on the radius R_{vertex} was dropped.
- The condition $|\Delta z| < 7$ cm was changed to $|\Delta z| < 4$ cm.

The measured value of the baryon asymmetry shows stability with respect to these variations of the selection criteria. Our final result for the baryon asymmetry is

$$A_B = (8.0 \pm 1.0 \pm 2.5)\% \,. \tag{3}$$

In order to study the dependence of the baryon asymmetry value on the proton polar angle and momentum, the whole procedure has been repeated in bins of $\cos(\theta)$ and p. The results of the measurements are shown in Fig. 7, where the error bars represent the sum of statistical and systematic uncertainties. Within the given momentum and angular intervals a decrease with the proton momentum as well as no significant angular dependence are observed for the baryon asymmetry. However, the size of the errors is too large to make definitive conclusions on the angular and momentum dependence of the observed baryon asymmetry.

However, the available statistics of identified protons and antiprotons allow to study the baryon asymmetry as function of the event properties. In the present paper we study A_B as function of the number of accompanying charged particles, N_{ch}^{obs}, measured within the same angular interval as the protons, $|\cos(\theta)| < 0.8$. The charged particles are required to originate from the common event vertex. Fig. 8(a) shows the measured distribution of N_{ch}^{obs} in the selected data sample. An average value of $\langle N_{ch}^{obs} \rangle$ is found to be in a good agreement with the average number of charged particles within the same angular interval in non–diffractive photoproduction events (about 4.5) [14]. Fig. 9(a) shows the values of A_B in bins of N_{ch}^{obs} as obtained from the fit of the DCA spectra and by correcting for the residual background contributions and the difference in the absorption cross sections for p and $\bar{p}$. The error bars in Fig.9(a) represent statistical uncertainties only. The systematic uncertainties discussed above depend only on the baryon properties and affect only the global normalisation in Fig 9(a). An additional point-to-point systematic error in Fig.9(a) might emerge if the kinematical properties of the analysed tracks change with the multiplicity N_{ch}^{obs}. Fig. 8(b-d) presents a comparison of vertex z-position, proton momentum and proton angular distributions for the whole data sample and for the subsample of events with $N_{ch}^{obs} > 9$. There is no significant difference observed for high multiplicity events in the particle spectra and the point-to-point part of the systematic error for the measured $A_B(N_{ch}^{obs})$ is therefore considered to be negligibly small. The measured dependence of the baryon asymmetry on N_{ch}^{obs} is stable under the variations of the selection conditions discussed above.

As an additional systematic cross check, the asymmetry in charged pion production has also been measured as function of N_{ch}^{obs}. The pions were identified and selected as described above. The result is presented in Fig. 9(b). Contrary to baryons, the pion asymmetry is compatible with being zero, and no dependence of the asymmetry on the multiplicity of accompanying charged particles is observed for pions.

4 Conclusions

A non–vanishing baryon asymmetry has been measured in the photoproduction at an average photon proton center of mass energy $W = 200$ GeV and at a distance of about 7 units in rapidity from the leading baryon production region. The baryon asymmetry in the photoproduction of protons and antiprotons within the momentum interval $0.3 < p < 0.6\ GeV/c$ and $|\cos(\theta)| < 0.8$ in the HERA laboratory frame is measured to be $A_B = 8.0 \pm 1.0(stat) \pm 2.5(sys)\%$. No significant dependence of the baryon asymmetry value on the proton polar angle and momentum has been found. The baryon asymmetry grows with increase of the number of charged particles accompanying the baryon production.

5 Acknowledgements

We are grateful to the HERA machine group whose outstanding efforts have made and continue to make this experiment possible. We thank the engineers and technicians for their work constructing and now maintaining the H1 detector, our funding agencies for financial support, the DESY technical staff for continual assistance and the DESY directorate for the hospitality which they extend to the non-DESY members of the collaboration. We have benefited from a number of stimulating discussions with B. Kopeliovich.

References

[1] Y.Eylon and H.Harari, Nucl. Phys. **B80** (1974) 349.

[2] B.Alper et al., Nucl. Phys. **B100** (1975) 237.

[3] T.Akesson et al., Nucl. Phys. **B228** (1983) 409.

[4] NA35 Collaboration, H.Ströbele et al., Nucl. Phys. **A525** (1991) 59.

[5] B.Z.Kopeliovich and B.G.Zakharov, Z. Phys. **C43** (1989) 241.

[6] B.Z.Kopeliovich, Sov. J. Nucl. Phys. **45** (1987) 1078.

[7] A.Capella and B.Z.Kopeliovich, Phys. Lett. **B381** (1996) 325.

[8] B.Z.Kopeliovich and B.Povh, Z. Phys. **C75** (1997) 693.

[9] EMC Collaboration, M.Arneodo et al., Z. Phys. **C35** (1987) 433.

[10] H1 Collaboration, I.Abt et al., Nucl. Instr. and Meth. **A386** (1997) 310 & 348.

[11] G.P.Eliseev, V.K.Kosmachevskii and V.A.Lubimov, Doklady Akad. Nauk SSSR **90** (1953) 995;
H1 Collaboration, "Antideuteron Production at HERA and Search for Heavy Stable Charged Particles", contributed paper to this conference;
H1 Collaboration, I.Abt et al., Nucl. Instr. and Meth. **A386** (1997) 310 & 348.

[12] R.Brun et al., *GEANT 3 User's Guide*, CERN-DD/EE **84-1**, Geneva (1987)

[13] R. Marshall et al., Phys. Rev. **91** (1953) 767;
H.Aihara et al., Nucl.Phys. **A360** (1981) 291;
V.N.Afonas'ev et al., Yad.Fiz. **40** (1984) 22;
K.Nakamura et al., Phys. Rev. Lett. **52** (1984) 731;
M. Sakitt et al., In Durham 1984, Proceedings, Antiproton 1984, 205.

[14] H1 Collaboration, C.Adloff et al., Z. Phys. **C76** (1997) 213.

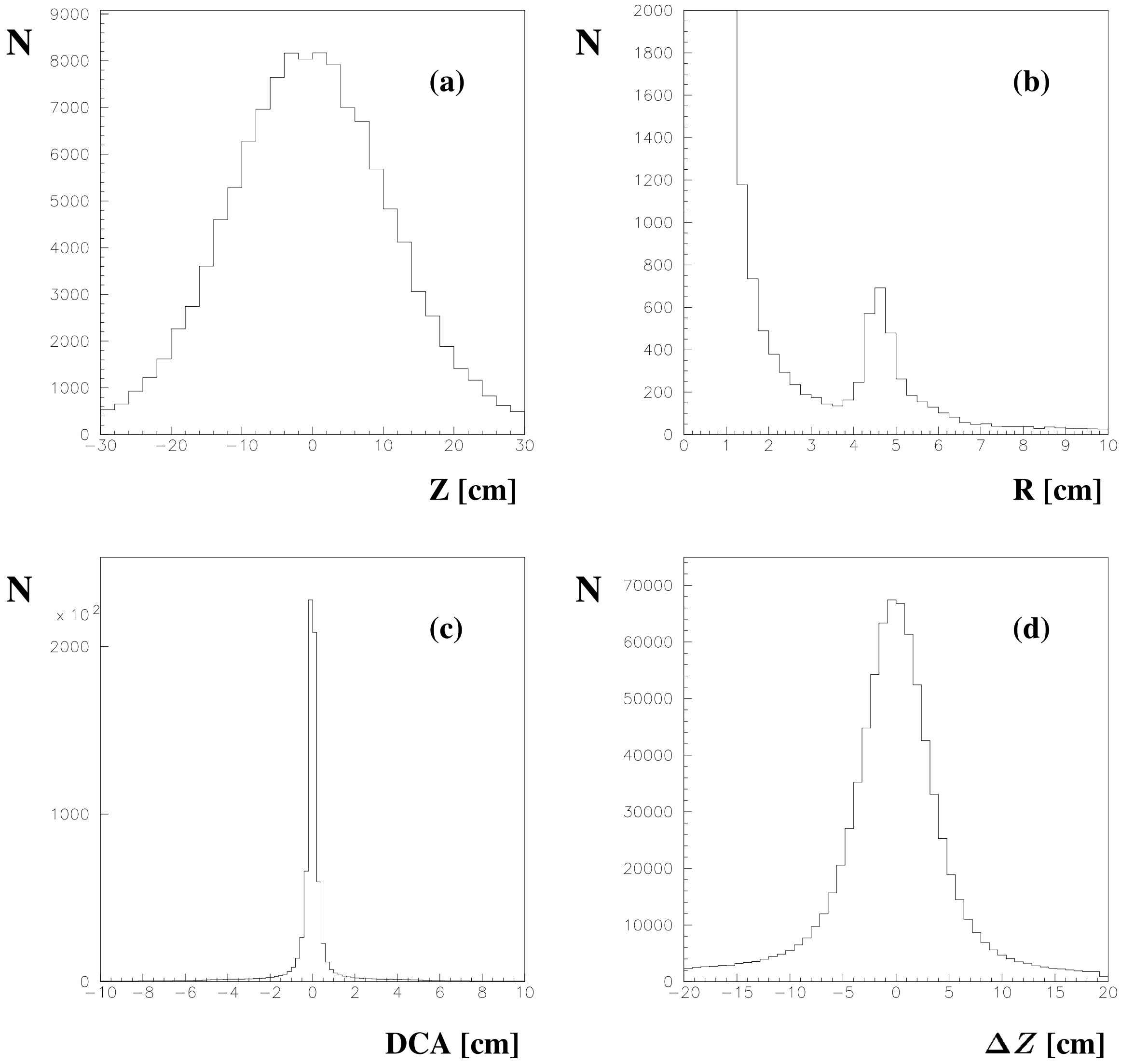

Figure 1: Measured z-position (a) and radius (b) of the reconstructed event vertex. Track distance of closest approach to the common vertex in the plane transverse to the beam direction, DCA (c) and along the z direction, Δz (d).

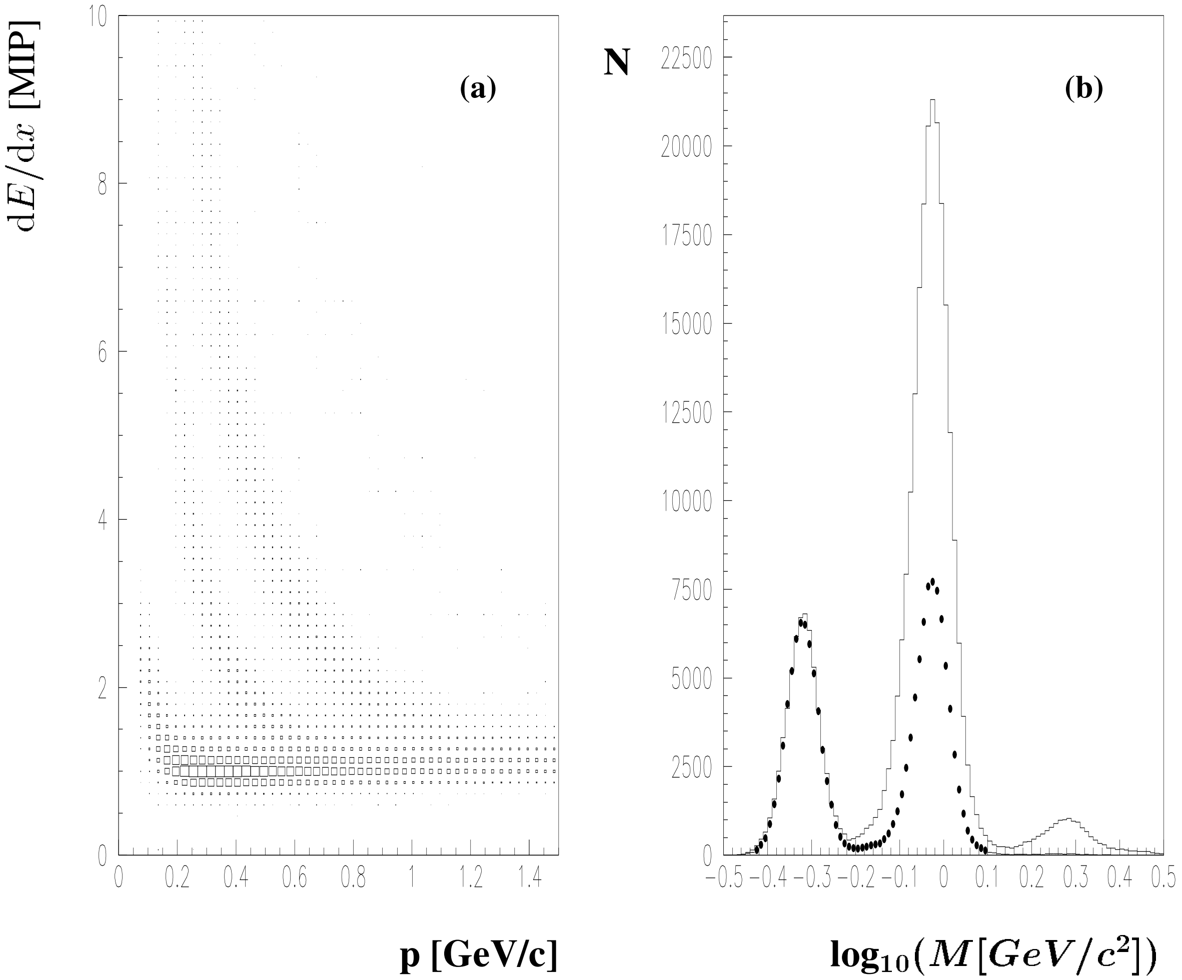

Figure 2: (a) – Observed energy loss versus momentum for positive and negative tracks in a sample of about 20,000 multi–hadron events. (b) – Logarithm of the particle mass as reconstructed from the simultaneous measurement of the momentum and the energy loss of the particle. Positively charged particles are shown by the histogram, while the negative particles are given by the full circles with error bars.

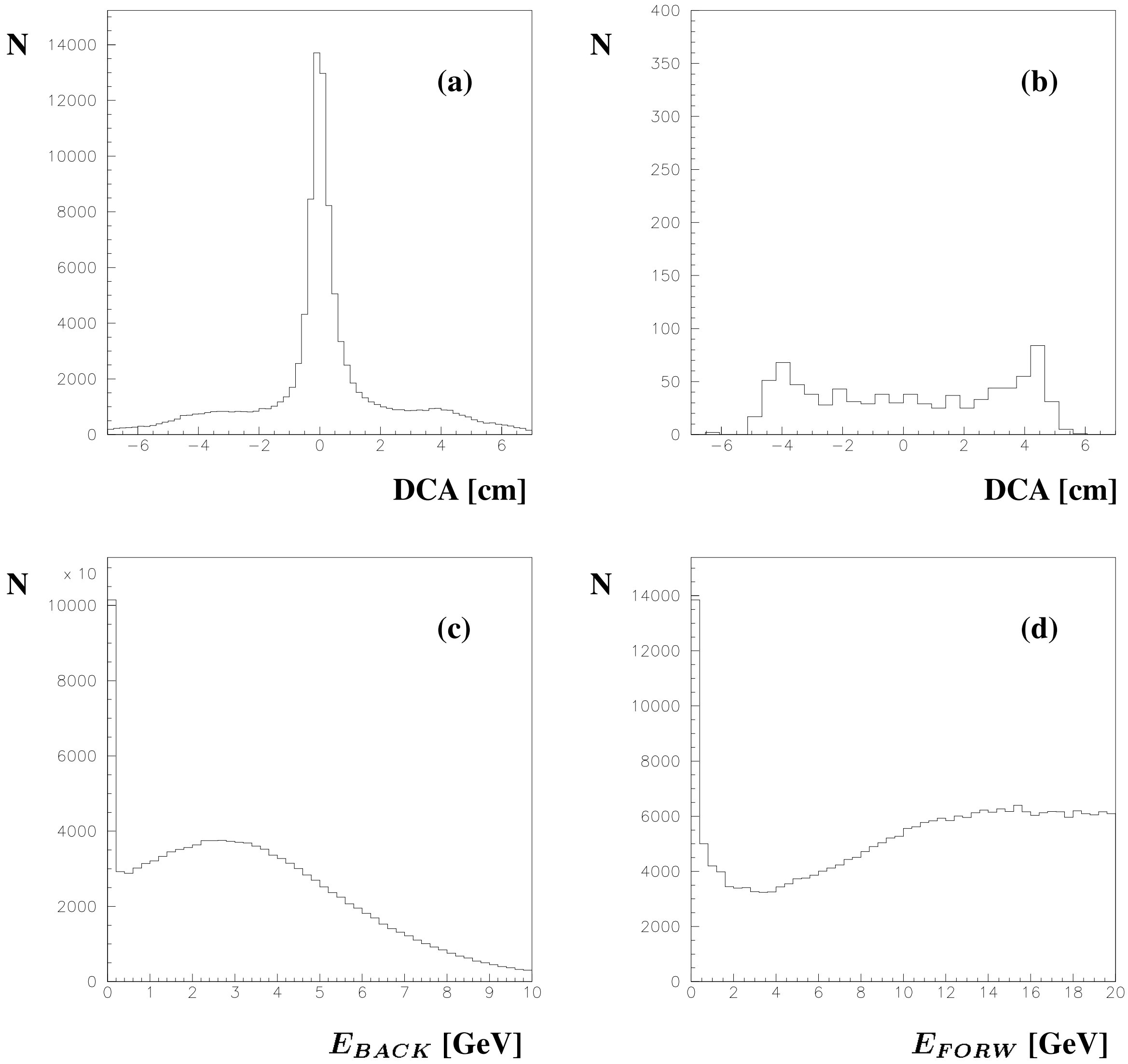

Figure 3: (a) – Measured DCA distribution for the identified protons in the data. (b) – Result of the Monte Carlo calculation of the DCA distribution for protons produced in the detector material around the interaction region. (c) – Energy spectrum measured in the Spacal calorimeter in the selected multi–hadron events. (d) – Energy spectrum measured in the LAr calorimeter ($\theta < 30°$) in the multi–hadron events.

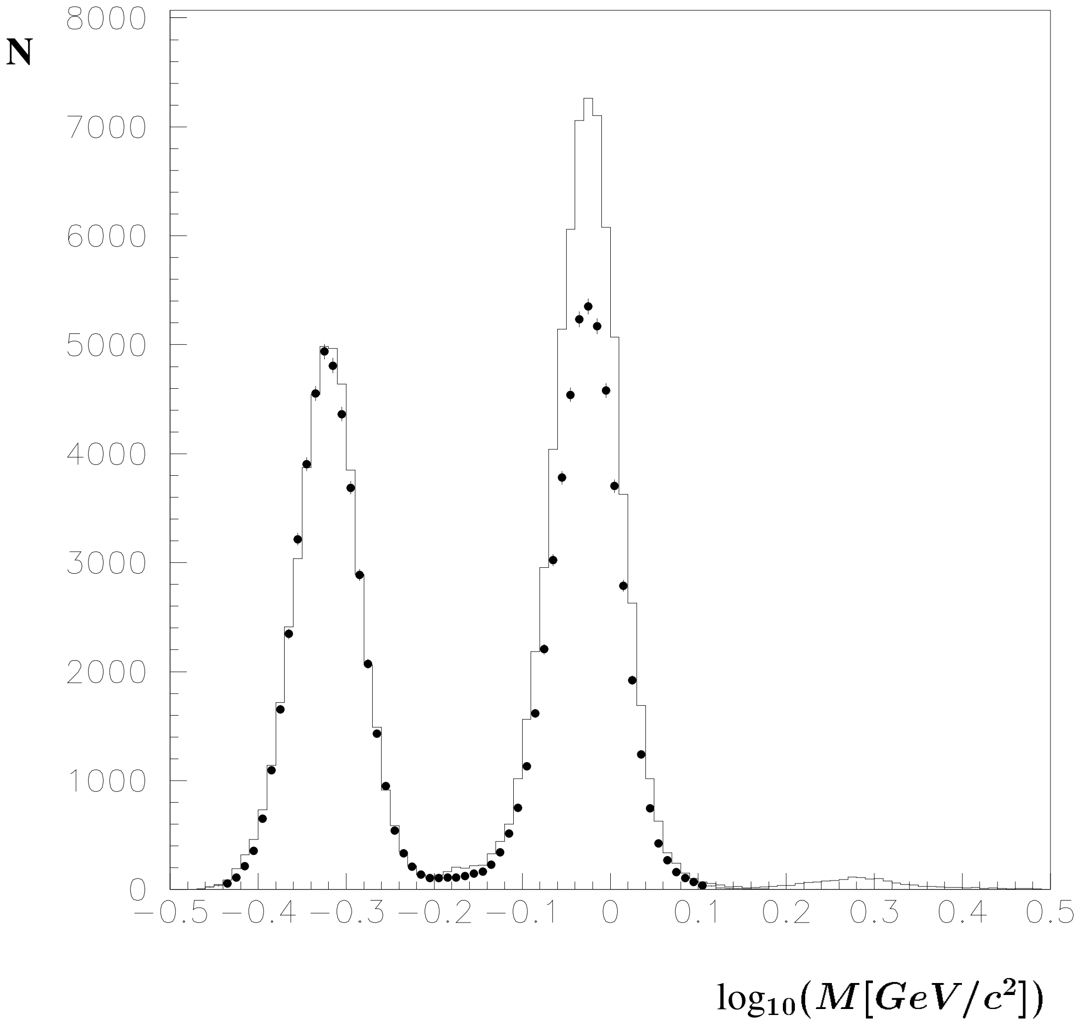

Figure 4: Logarithmic mass distributions for tracks originating from the common event vertex after background suppression. Positively charged particles are shown by the histogram, negative particles are given by the full circles with error bars.

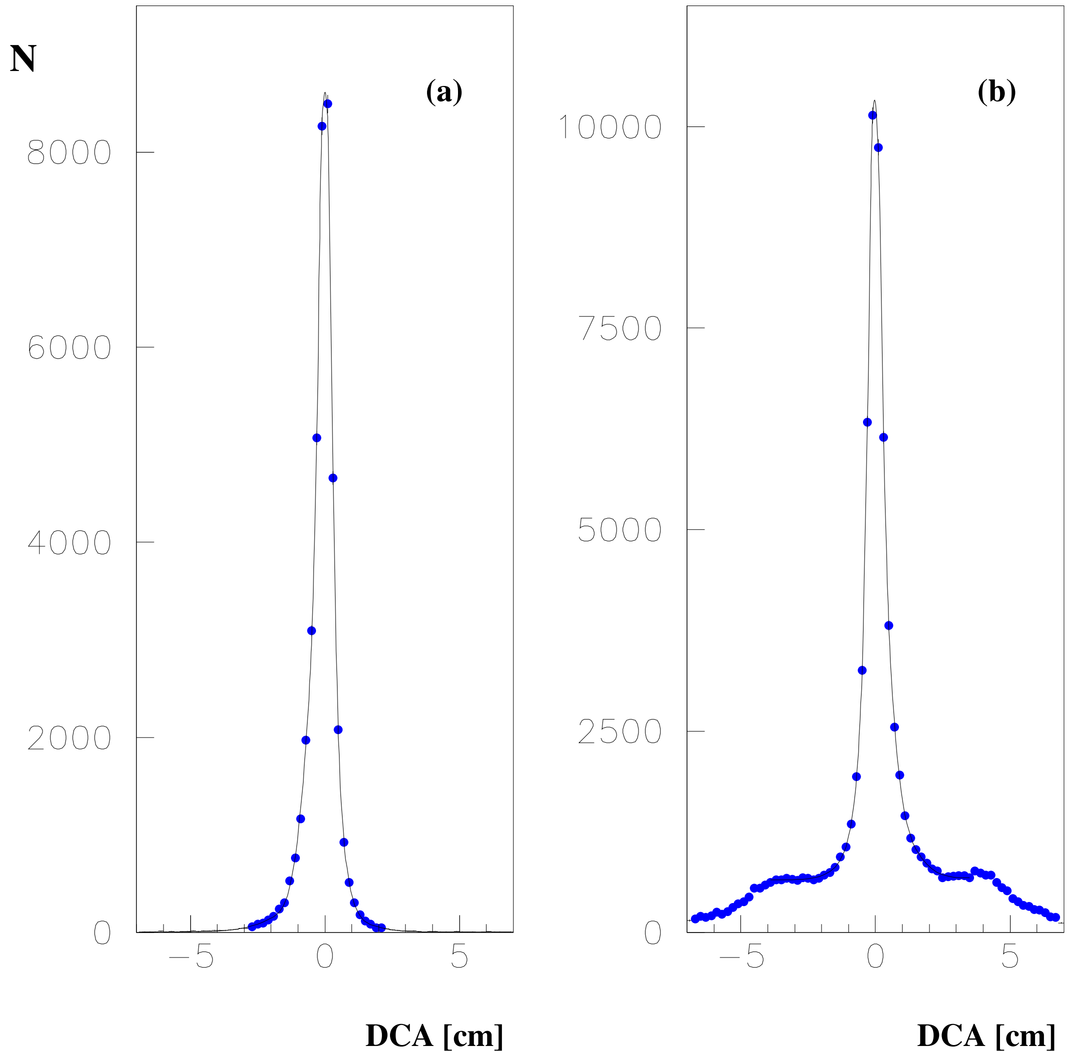

Figure 5: The measured DCA distributions for negatively (a) and positively (b) charged particles with a value of $\log_{10}(M)$ lying within a window of ± 0.1 around the nominal value for the proton mass. The curves show the results of the fits described in the text.

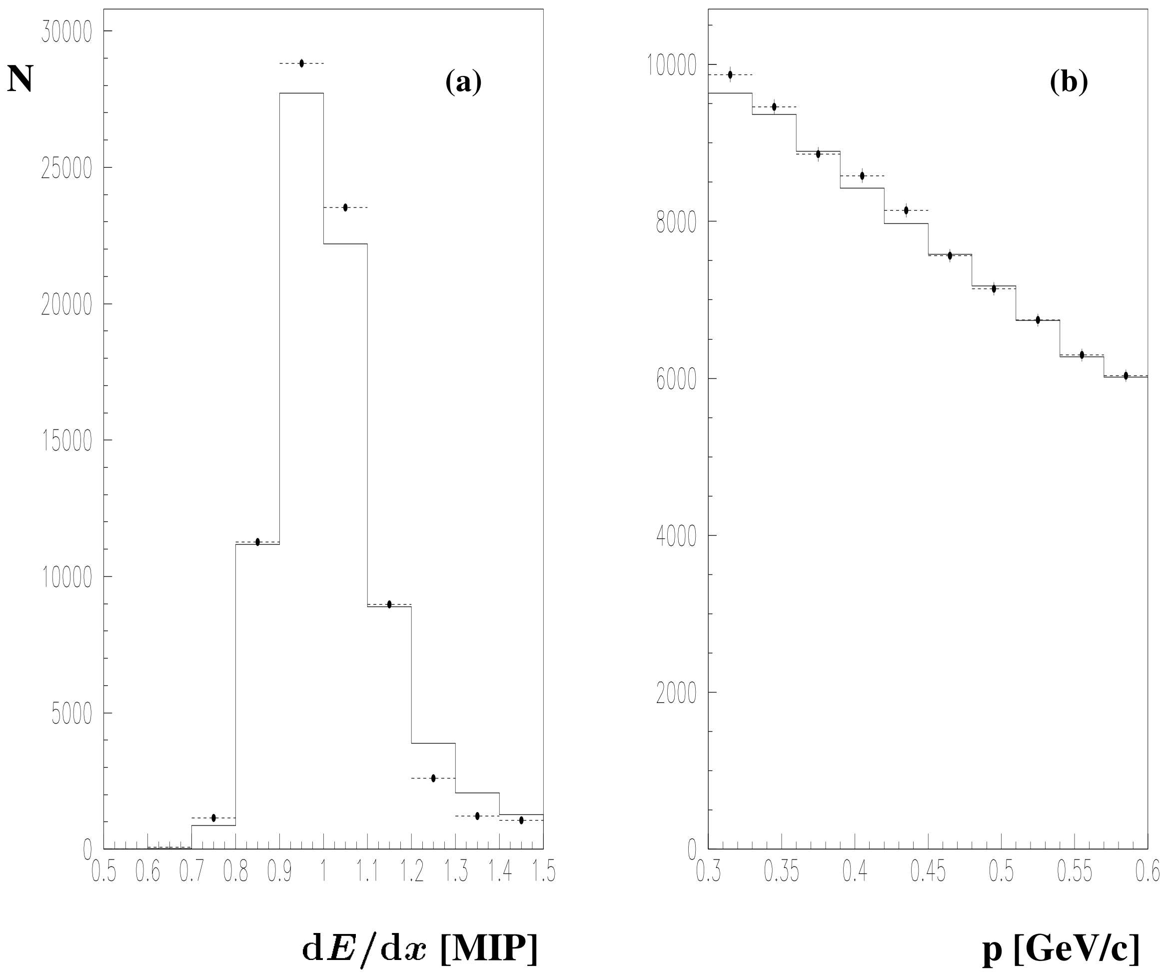

Figure 6: Measured $\mathrm{d}E/\mathrm{d}x$ (a) and momentum (b) distributions for positive (points) and negative (histogram) pions.

H1 Preliminary

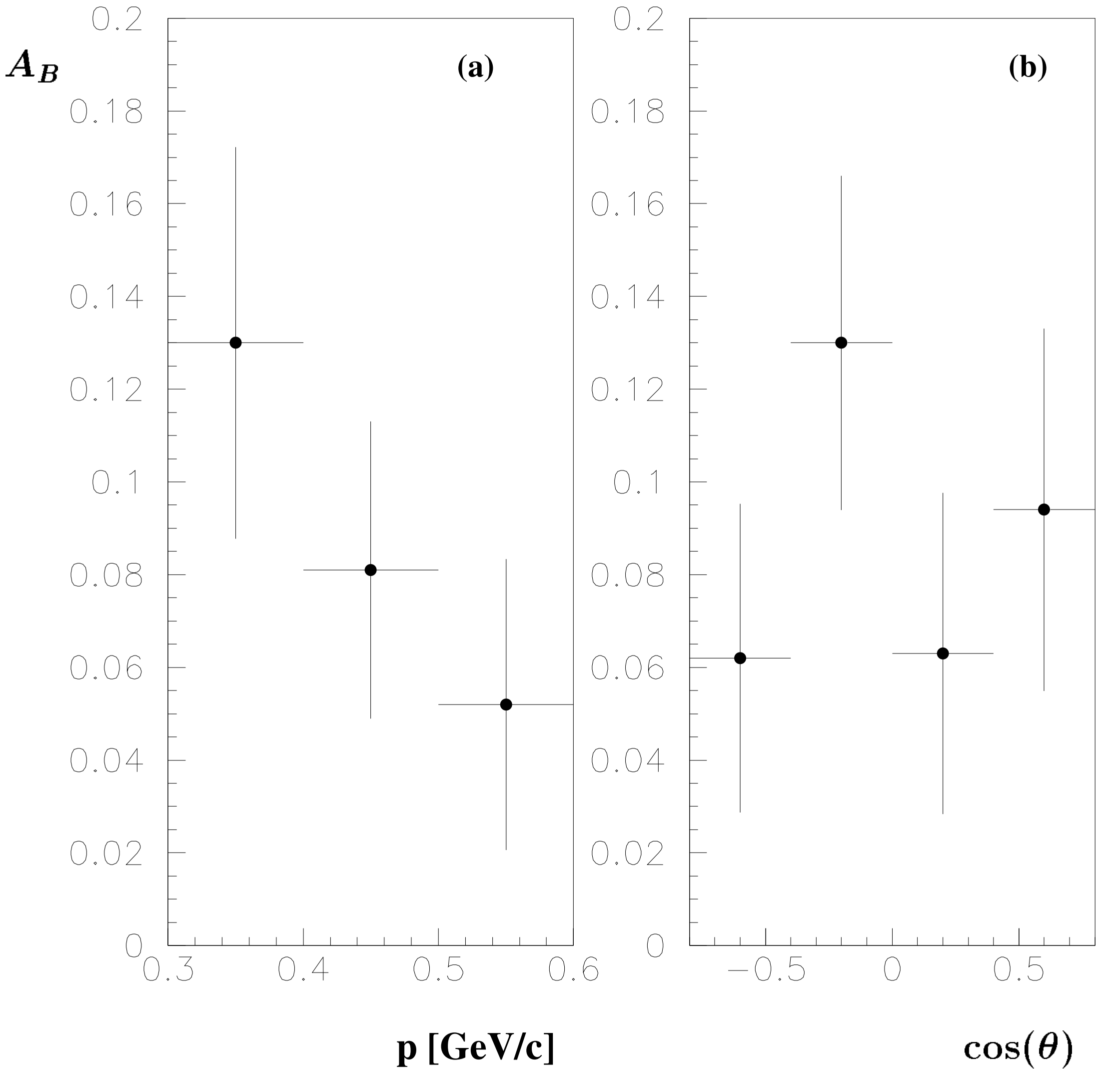

Figure 7: Baryon asymmetry as function of the proton momentum (a) and the polar angle (b).

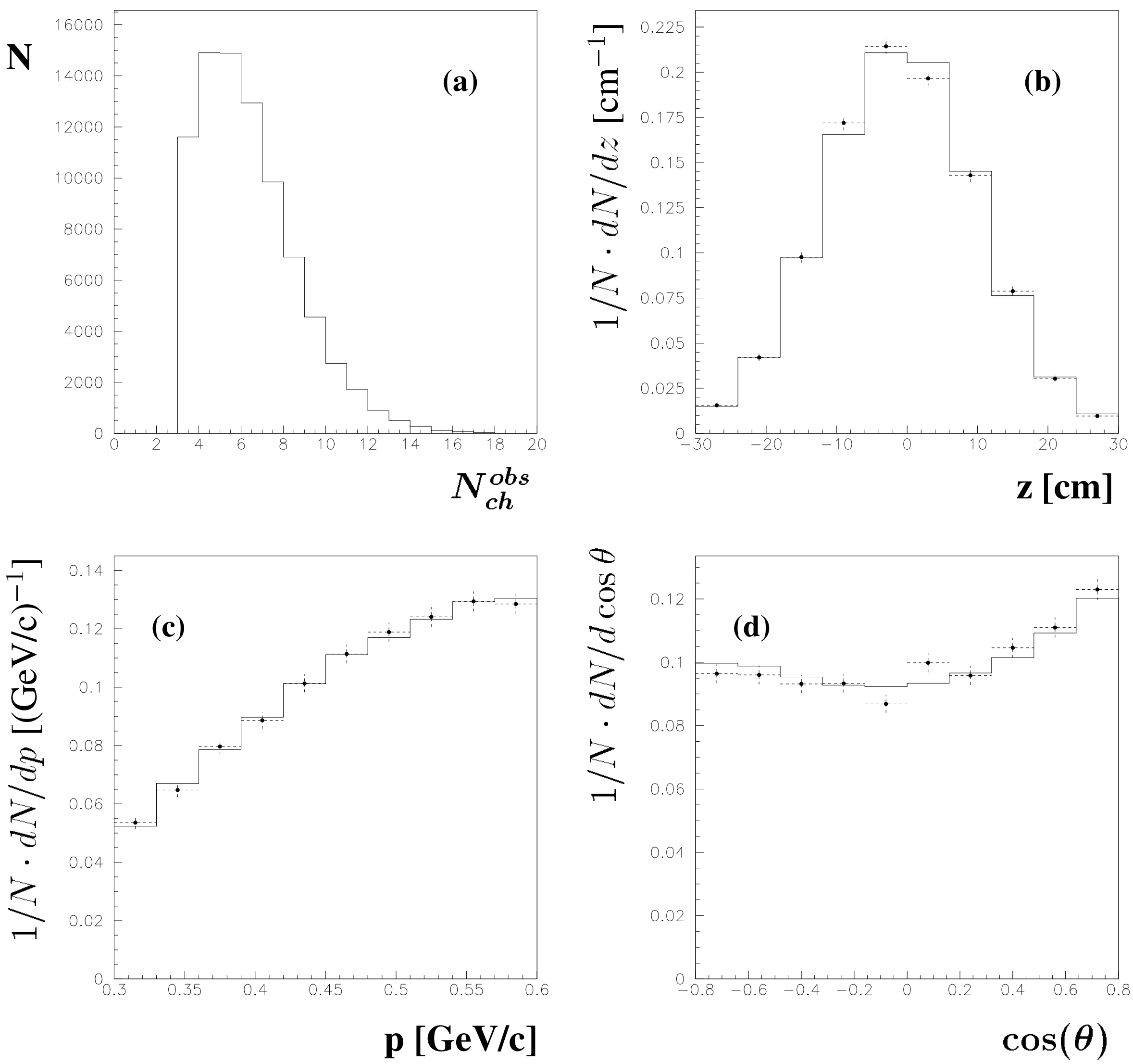

Figure 8: (a) – Charged particle multiplicity within the angular interval of the proton measurement. (b-d) – Comparison of the measured vertex z-position, proton momentum and polar angule distributions for the whole data sample (histograms) and for a subsample of events with $N_{ch}^{obs} > 9$ (points with error bars).

H1 Preliminary

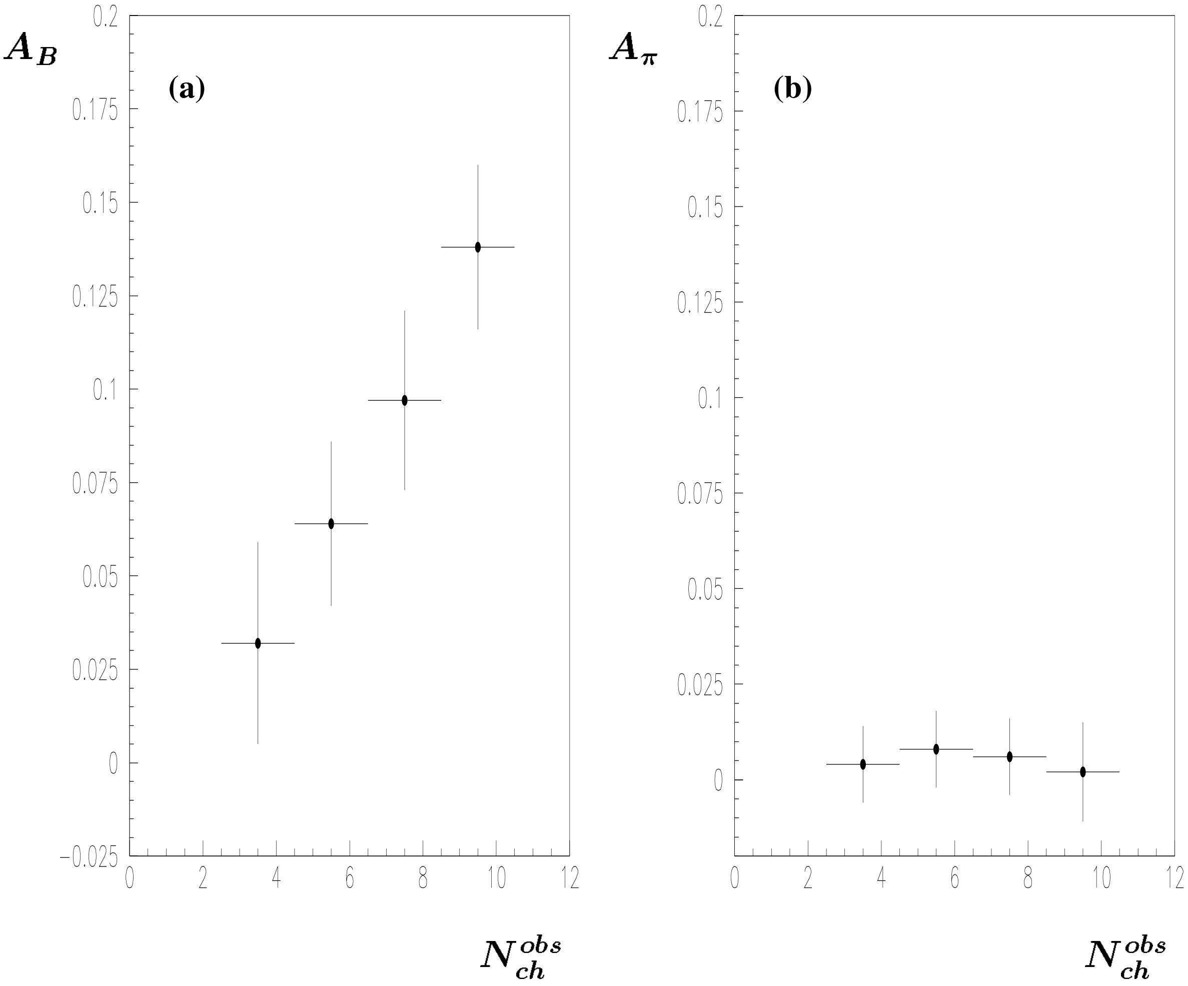

Figure 9: Baryon (a) and charged pion (b) asymmetry as function of the number of accompanying charged particles N_{ch}^{obs} measured within the same angular interval as the baryons, in non-diffractive photoproduction at 200 GeV CM energy.